Throwing a knife

Dhairya Shah (wylited)
Analysis and Approaches HL

Internal Assessment: Mathematical Exploration
Examination Session: May 2025

An investigation into the modelling of the flight of the tip of a knifes blade in relation to its center of mass as a graph

Contents

1. Introduction

Lacking hobbies in my 18th year of existence, I decided to pick up knife throwing at a local range. Unlike what is shown in the movies, it's a lot harder and rather unintuitive to throw a knife and get it to embed its tip into the target.

This is because a throwing knife is typically thrown with spin, causing the tip to rotate throughout its flight. Since the likelihood of the knife embedding itself into a block is dependent on angle of the tip against the normal surface of the target, there is a very narrow range of angle at which the knife tip can successfully penetrate the target, making precise control required for a successful throw.

Professionals, in contrast to me, have years of experience and an inherent intuition of how the knife will spin and move through the air towards a target. This enables them to land their knifes perfectly every single time. I, on the other hand, can only cause blunt force trauma to my target as the handle smacks them.

To deepen my understanding of knife throwing without actually practicing at the range. I will be attempting to model the trajectory of a throwing knife and its rotating tip to understand how the initial conditions in which I throw a knife impacts its success in landing in the target.

2. Analysis and Exploration

2.1. Initial Understanding

Definition 2.1. The geometric center or **centroid** for any object is the arithmetic mean position of all points in the object.

Since a typical throwing knife is balanced, their **center of gravity** and its geometrical **centroid** are equivalent. The implications of this is that the throwing knife will rotate around its center of gravity. Thus the furthest point A, being the tip of the knife's blade OA, will trace a circle when rotated.

We can visualize what will happen as focus of the circle moves away from the origin O while the knife is rotating, where l is the radius, x is the horizontal displacement, y is the vertical displacement, and α is the angle of rotation.

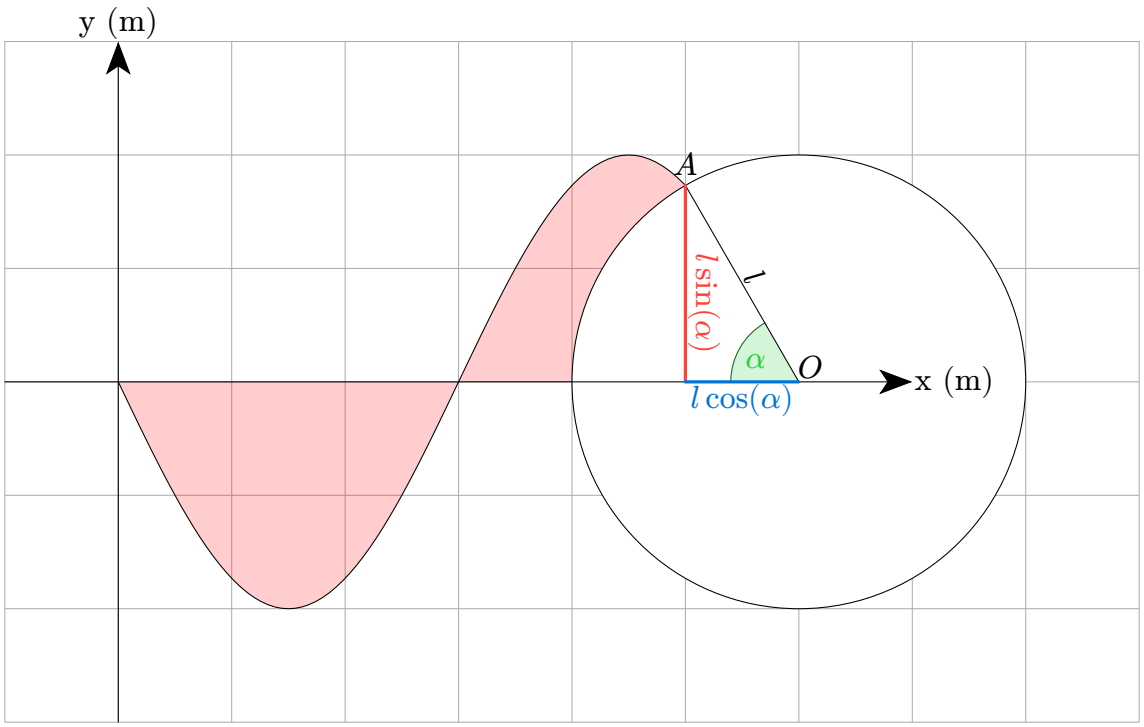

Figure 1: The path that a rotating point on a circle traces during horizontal displacement.

It is clear that this graphs a sinusoidal wave in the shape of the sine function, $y = \sin(x)$. However, we need to note that sine will not be the correct function to model the behaviour. This is because at $t = 0, \sin(t) = 0$, this doesn't make sense as the blade tip is always offset from the center of mass. Thus we should use invert them and use a cosine function instead.

Theorem 2.2. The path traced by the tip of a rotating knife blade in flight follows a sinusoidal wave pattern similar to the cosine function.

2.2. Describing the Flight Path as a Vector

The flight path is the line that the center of mass would trace in space.

Using an equation to describe the flight path such as $y = 0$ is inherently limited because the equation only encodes a set of pairs of coordinates (x, y).

In order to model the system, our model should aim to encode more information to improve accuracy and nuance of the model.

To achieve this, we can use vector to encode additional data.

Definition 2.3. Let $\vec{r}(t)$ be a vector-valued function representing a line in the xy plane. The general vector form of a line can be expressed as

$$\vec{r}(t) = v_0 + tv \tag{1}$$

Where $v_0 = \begin{bmatrix} x_0 \\ y_0 \end{bmatrix}$ is a point on the line (the position vector), $v = \begin{bmatrix} a \\ b \end{bmatrix}$ is a non-zero vector parallel to the line (the direction vector), and $t \in \mathbb{R}$ is the parameter.

Example 2.4. Consider a line parallel to the x-axis passing through the point $(0, k)$ where $k \in \mathbb{R}$. Such a line can be represented by choosing $v_0 = \begin{bmatrix} 0 \\ k \end{bmatrix}$ and $v = \begin{bmatrix} 1 \\ 0 \end{bmatrix}$

Therefore:

$$\begin{aligned} \vec{r}(t) &= \begin{bmatrix} 0 \\ k \end{bmatrix} + t\begin{bmatrix} 1 \\ 0 \end{bmatrix} \\ &= \begin{bmatrix} t \\ k \end{bmatrix} \end{aligned} \tag{2}$$

This parametric representation generates all points (x, k) on a line parallel to the x-axis at height k.

Furthermore, the parameterisation with the variable t naturally extends our model to kinematic analysis, where t would represent time. This allows us to express more dynamic properties of the line such as speed.

2.3. Modelling the Knife's Tip in Flight

Currently, to describe a cosine wave we use the following equation $y = \cos(x)$

In order to vectorize this, we can refer back to Figure 1, which shows that in the sine function, at angle α, the y displacement is $\cos(\alpha)$ and the x displacement is $\sin(\alpha)$.

However, in this scenario, our angle will vary with time t and an angular frequency ω.

Definition 2.5. Angular Frequency ω is the rate of change in angle per unit time, measured in radians per second ($\frac{\text{rad}}{s}$).

This is used to describe the "speed" at which something rotates.

It follows that ωt will always result in an angle.

So we can vectorize the displacement that the cosine function represents with $\vec{c}(t)$.

$$\vec{c}(t) = \begin{bmatrix} \cos(\omega t) \\ \sin(\omega t) \end{bmatrix} \tag{3}$$

In our context, once the knife is released, the rate of rotation ω does not change and thus is an initial condition of our model.

Thus, we can take our base flight path $\vec{r}(t) = \begin{bmatrix} t \\ k \end{bmatrix}$, and simply add the vector of cosine wave displacement scaled to the length of the blade l in order to model the tip.

$$\begin{aligned} \overrightarrow{r_{\text{tip}}}(t) &= \vec{r}(t) + l\vec{c}(t) \\ &= \begin{bmatrix} t \\ k \end{bmatrix} + l\begin{bmatrix} \cos(\omega t) \\ \sin(\omega t) \end{bmatrix} \\ &= \begin{bmatrix} t + l\cos(\omega t) \\ k + l\sin(\omega t) \end{bmatrix} \end{aligned} \tag{4}$$

We can graph this to verify that our $\overrightarrow{r_{\text{tip}}}(t)$ function is correct.

Definition 2.6. To graph a vector-valued function with a parameter $\vec{r}(t) = \begin{bmatrix} a(t) \\ b(t) \end{bmatrix}$, we plot the points (x, y) where $x = a(t)$ and $y = b(t)$ as t varies over its domain.

Thus to graph $\text{tip}(t) = \begin{bmatrix} t + l\cos(\omega t) \\ k + l\sin(\omega t) \end{bmatrix}$, we take the equations

$$\begin{aligned} x &= t + l\cos(\omega t) \\ y &= k + l\sin(\omega t) \end{aligned} \tag{5}$$

Where our initial conditions k, ω, and l are arbitrary constants 0, 1 and 1 for now.

$$\begin{aligned} x &= t + l\cos(t) \\ y &= l\sin(t) \end{aligned} \tag{6}$$

We can graph this for $0 < t < 20$

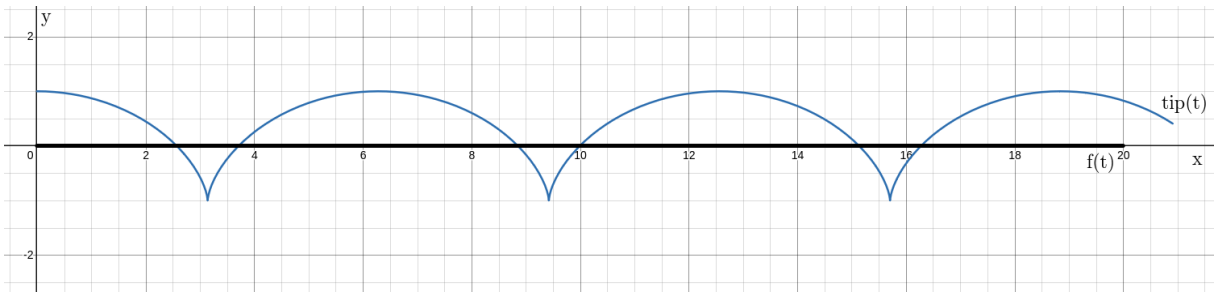

Figure 2: The graph of $\overrightarrow{r_{\text{tip}}}(t)$ and $\vec{r}(t)$

This graph is strikingly odd - instead of graphing a sinusoidal wave, we get a periodic bump-like pattern.

This graph provides conflicting evidence to our initial Theorem 2.2 predicting the sinusoidal nature of the path. Instead of the expected wave pattern, we observe a distinctly different periodic curve.

These curves are quite recognizable as cycloids, reminiscent of the trajectories traced by charged particles under perpendicular electric and magnetic fields ($E \times B$ drift) that we studied in physics.

2.4. Analysis of the Cycloid

Our initial reasoning seemed logical - a rotating point on a moving circle should trace a sine wave, as a sine wave represents the vertical position of a point rotating in a circle.

However, this overlooks a key difference:

$$\begin{aligned} &\text{Sine wave:} \quad x = t && y = \sin(t) \\ &\text{Our model:} \quad x = t + \cos(t) && y = \sin(t) \end{aligned} \tag{7}$$

The $t + \cos(t)$ term reveals that our horizontal position combines both forward motion (t) and rotation ($\cos(t)$). Unlike a sine wave where horizontal motion is independent of rotation, our model shows these components are coupled.

This mathematical analysis reveals what our intuition missed: the true path is a cycloid - the curve traced by a point on a rolling circle. By using a vector-valued function with parameter t, we can accurately represent this more complex motion, including points where the path crosses itself.

Theorem 2.7. The path traced by the tip of a rotating knife blade in flight follows a cycloid pattern, described by the vector valued function: $\overrightarrow{r_{\text{tip}}}(t) = \vec{r}(t) + l\vec{c}(t)$ where $\vec{r}(t)$ is the flight path, $\vec{c}(t) = \begin{bmatrix}\cos(\omega t)\\ \sin(\omega t)\end{bmatrix}$, l is the length of the blade, t is time, and ω is the angular frequency of rotation

Proof of Theorem 2.7. As demonstrated by our vector analysis, the tip's position is the sum of:

1. The motion of the center of mass: $\begin{bmatrix}t\\ k\end{bmatrix}$
2. The rotational displacement: $\begin{bmatrix}\cos(\omega t)\\ \sin(\omega t)\end{bmatrix}$
3. The scalar displacement of the tip: l

This combination necessarily produces a cycloid, as verified by our graphical analysis. □

2.5. Deriving an Accurate Flight Path

Currently our flight path is completely abstract. To model more real world characteristics, we can attempt to integrate an angle of release θ.

To achieve this, we can could use a transformation matrix, which when multiplied against a vector valued function, will transform our flight path and cycloid function.

Specifically we need to make use of a rotation matrix, which is a transformation matrix that rotates a set of points around the origin.

Theorem 2.8. The rotation matrix to rotate points in the xy plane counterclockwise through an angle θ about the origin is

$$R = \begin{bmatrix}\cos(\theta) & -\sin(\theta)\\ \sin(\theta) & \cos(\theta)\end{bmatrix} \tag{8}$$

Proof of Theorem 2.8. Consider a new rotated xy plane with axes rx and ry.

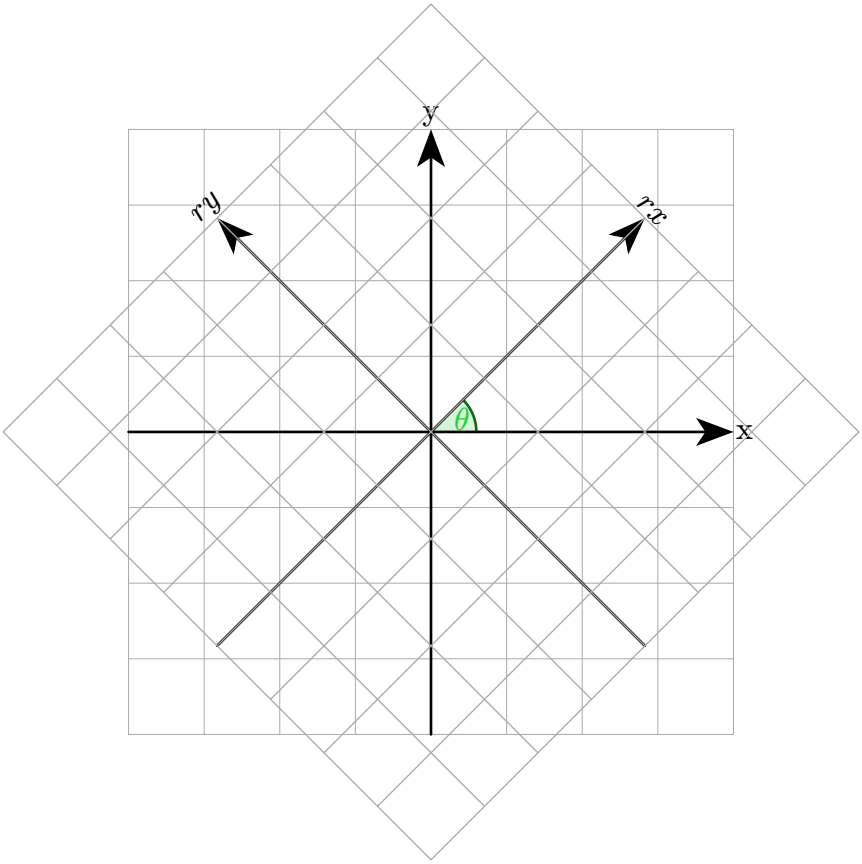

Figure 3: Rotated plane xy

We can compare our xy plane's unit vectors $\hat{\imath}$ and $\hat{\jmath}$ with the rotated $rxry$ plane's unit vectors $\hat{p}$ and $\hat{q}$

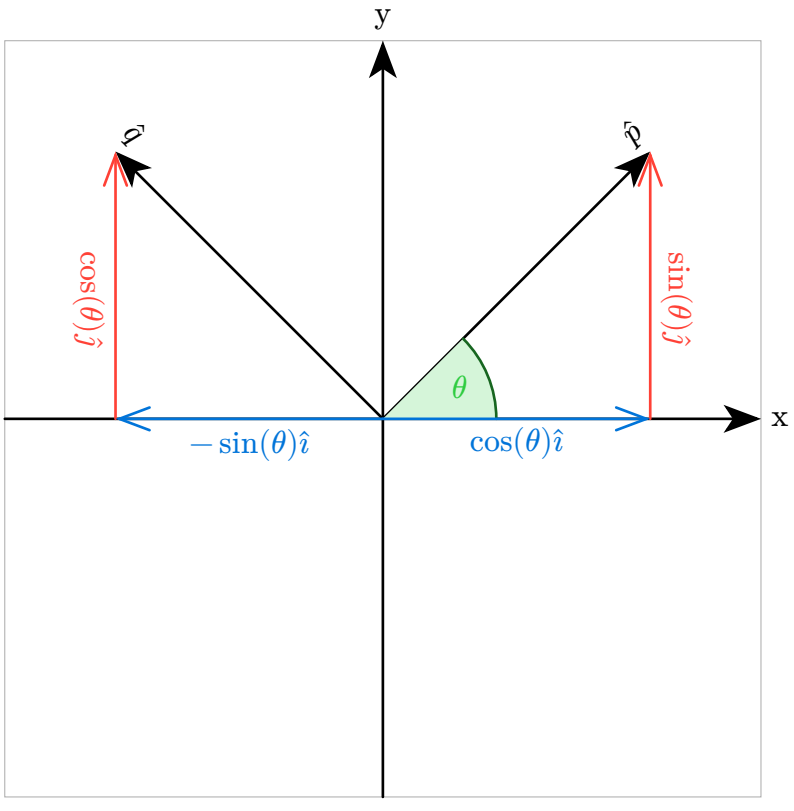

Figure 4: A unit movement in the rotated grid compared to the original plane xy

By using vector addition, we can define $\hat{p}$ and $\hat{q}$ given the angle of rotation θ.

$$\begin{aligned}\hat{p} &= \cos(\theta)\hat{\imath} + \sin(\theta)\hat{\jmath} \\ &= \cos(\theta)\begin{bmatrix}1\\0\end{bmatrix} + \sin(\theta)\begin{bmatrix}0\\1\end{bmatrix} \\ &= \begin{bmatrix}\cos(\theta)\\0\end{bmatrix} + \begin{bmatrix}0\\\sin(\theta)\end{bmatrix} \\ &= \begin{bmatrix}\cos(\theta)\\\sin(\theta)\end{bmatrix}\end{aligned} \tag{9}$$

$$\begin{aligned}\hat{q} &= \cos(\theta)\hat{\jmath} - \sin(\theta)\hat{\imath} \\ &= \cos(\theta)\begin{bmatrix}0\\1\end{bmatrix} - \sin(\theta)\begin{bmatrix}1\\0\end{bmatrix} \\ &= \begin{bmatrix}0\\\cos(\theta)\end{bmatrix} + \begin{bmatrix}-\sin(\theta)\\0\end{bmatrix} \\ &= \begin{bmatrix}-\sin(\theta)\\\cos(\theta)\end{bmatrix}\end{aligned} \tag{10}$$

Since the identity transformation matrix that does not transform $\hat{\imath}$ and $\hat{\jmath}$ is

$$[\hat{\imath}\ \ \hat{\jmath}] = \begin{bmatrix}1 & 0\\0 & 1\end{bmatrix} \tag{11}$$

We can determine the rotation matrix to be

$$R = [\hat{p}\ \ \hat{q}] = \begin{bmatrix}\cos(\theta) & -\sin(\theta)\\\sin(\theta) & \cos(\theta)\end{bmatrix} \tag{12}$$

We can verify this is correct by rotating the vector $\begin{bmatrix}t\\0\end{bmatrix}$ by $\theta = 30°$

$$\begin{aligned}\vec{g}(t) &= \begin{bmatrix}t\\0\end{bmatrix}\begin{bmatrix}\cos(\theta) & -\sin(\theta)\\\sin(\theta) & \cos(\theta)\end{bmatrix} \\ &= \begin{bmatrix}t\cos(\theta) + 0\sin(\theta)\\-t\sin(\theta) + 0\cos(\theta)\end{bmatrix} \\ &= \begin{bmatrix}t\cos(30°)\\-t\sin(30°)\end{bmatrix}\end{aligned} \tag{13}$$

Which we can parameterize to graph

$$\begin{aligned}x &= t\cos(30°)\\y &= -t\sin(30°)\end{aligned} \tag{14}$$

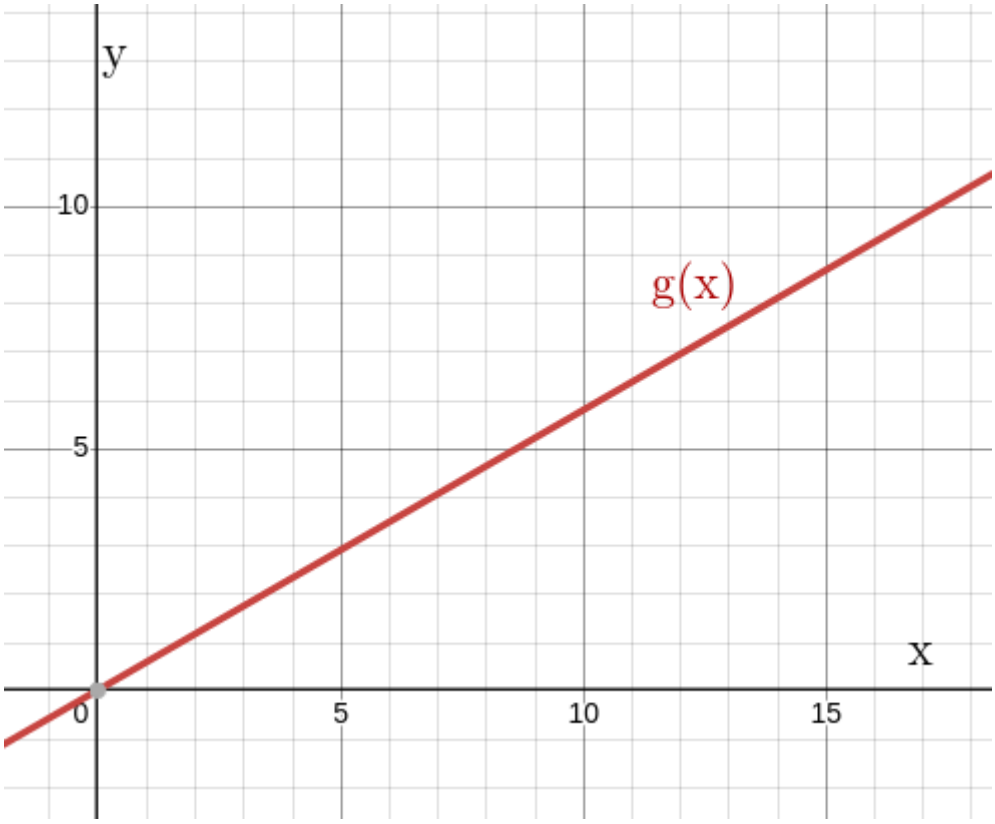

Figure 5: $\vec{g}(t)$, which is $\begin{bmatrix} t \\ 0 \end{bmatrix}$ rotated by 30°

□

We can verify again that our cycloidal vector function will apply on a rotated vector for its flight path.

$$\begin{aligned} \overrightarrow{r_{\text{tip}}}(t) &= \vec{g}(t) + l\vec{c}(t) \\ &= \begin{bmatrix} t\cos(30°) \\ -t\sin(30°) \end{bmatrix} + \begin{bmatrix} l\cos(\omega t) \\ l\sin(\omega t) \end{bmatrix} \\ &= \begin{bmatrix} t\cos(30°) + l\cos(\omega t) \\ -t\sin(30°) + l\sin(\omega t) \end{bmatrix} \end{aligned} \tag{15}$$

Parameterized

$$\begin{aligned} x(t) &= t\cos(30°) + l\cos(\omega t) \\ y(t) &= -t\sin(30°) + l\sin(\omega t) \end{aligned} \tag{16}$$

We can graph $\vec{g}(t)$ for $0 < t < 20, l = 1, \omega = 1$.

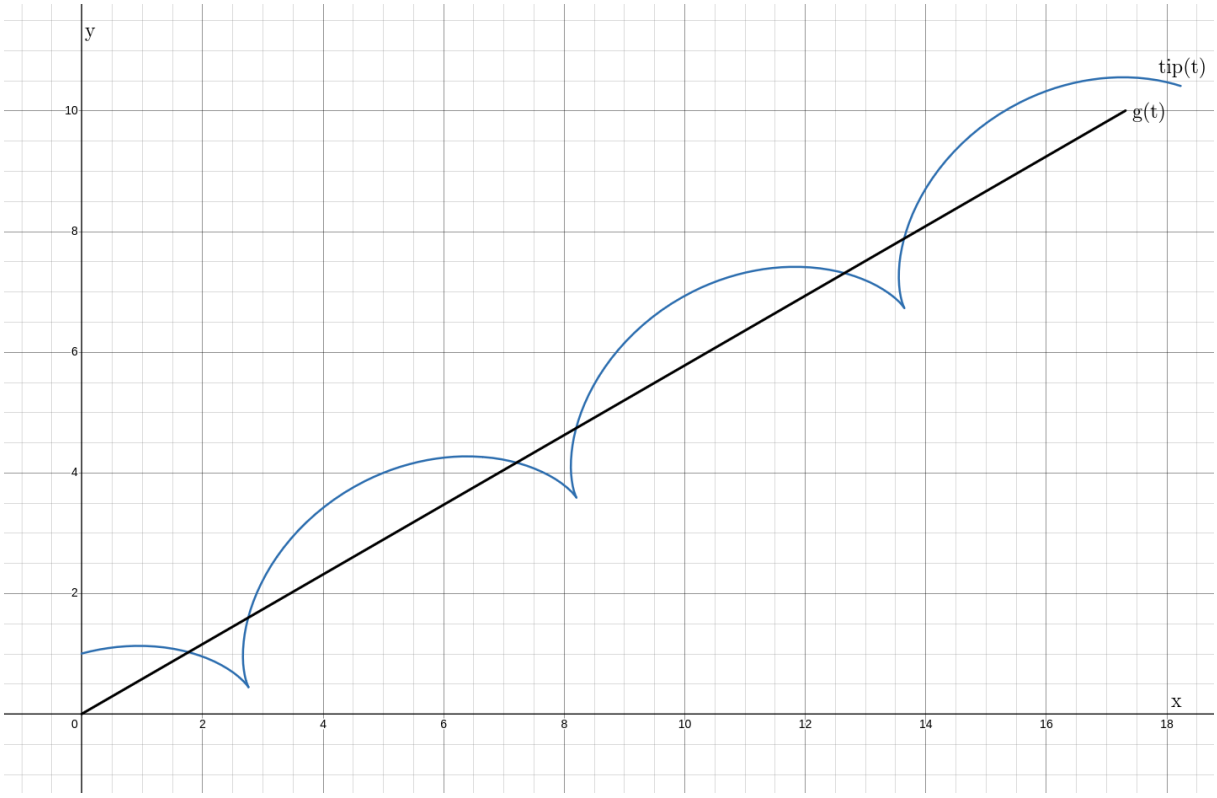

Figure 6: The graph of $\overrightarrow{r_{\text{tip}}}(t)$ and $\vec{g}(t)$

We can further develop our model by integrating initial velocity.

For a projectile released with initial velocity $\hat{v}$ at angle θ, we can decompose the motion into horizontal and vertical components. This decomposition is fundamental because:

- Horizontal motion occurs at constant velocity (neglecting air resistance)
- Vertical motion is subject to gravitational acceleration

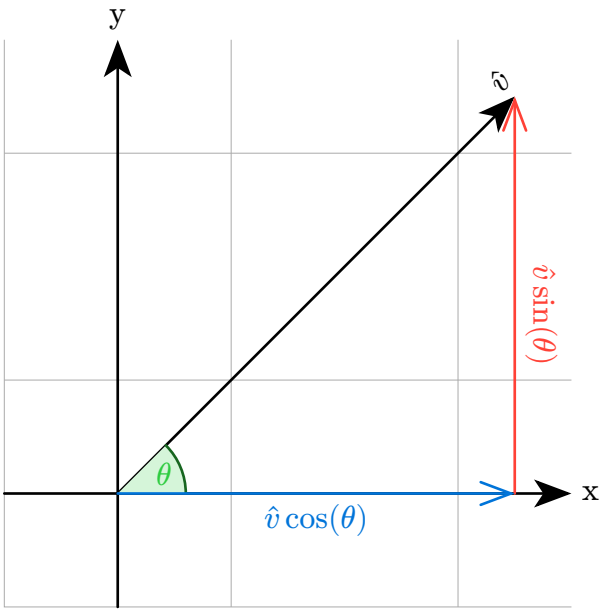

Figure 7: A velocity vector split into its x and y components given an angle θ

The initial velocity vector $\hat{v}$ can be resolved into its components using trigonometric functions.

- $x = \cos(\theta)\hat{v}$
- $y = \sin(\theta)\hat{v}$

Under constant gravitational acceleration $g = -9.81ms^{-2}$, we can derive the vector using the standard kinematic equations:

$$\vec{r}(t) = \begin{bmatrix} \cos(\theta)\hat{v}t \\ \sin(\theta)\hat{v}t - \left(\frac{1}{2}\right)9.81t^2 \end{bmatrix} \tag{17}$$

Parameterized

$$\begin{aligned} y(t) &= \sin(\theta)\hat{v}t - \left(\frac{1}{2}\right)9.81t^2 \\ x(t) &= \cos(\theta)\hat{v}t \end{aligned} \tag{18}$$

We can again graph the flight path and the tip path added on top of it to verify that our model still behaves as expected.

$$\begin{aligned} \overrightarrow{r_{\text{tip}}}(t) &= \vec{r}(t) + l\vec{c}(t) \\ &= \begin{bmatrix} \cos(\theta)\hat{v}t + l\cos(\omega t) \\ \sin(\theta)\hat{v}t - \left(\frac{1}{2}\right)9.81t^2 + l\sin(\omega t) \end{bmatrix} \end{aligned} \tag{19}$$

Graphing from $\overrightarrow{r_{\text{tip}}}(t)$ and $\vec{r}(t)$ $0 < t < 6$, with $\hat{v} = 10, l = 0.1, \omega = 10$

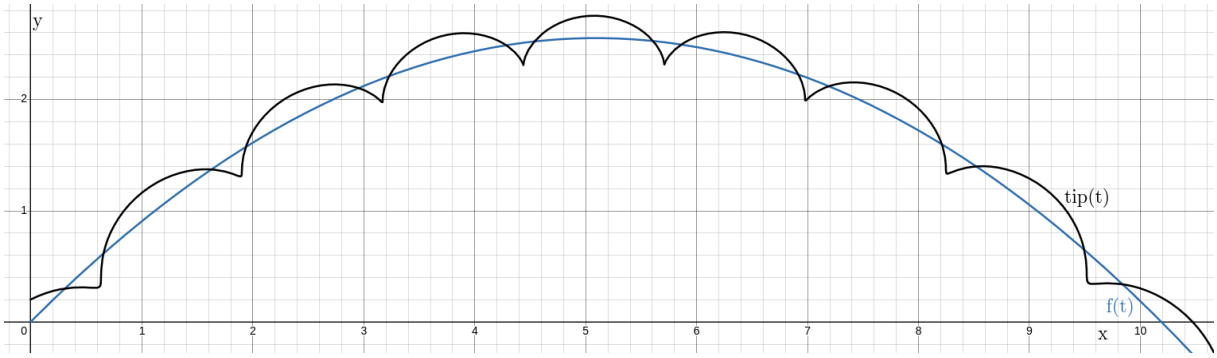

Figure 8: The graph of $\overrightarrow{r_{\text{tip}}}(t)$ and $\vec{r}(t)$

We can see that this is an extremely convincing model. We can now begin our final verification of our model.

2.6. Experimental Verification of the Model

In order to verify our model, we can throw a pen and record it. On the video, we can plot the center of mass and the tip of the pen every 0.1 seconds.

We can further extract the angular frequency and the initial velocity of the pen from the video and use it in our model.

Finally, we can overlay the image in desmos scaled accordingly and compare the models prediction and the traced path.

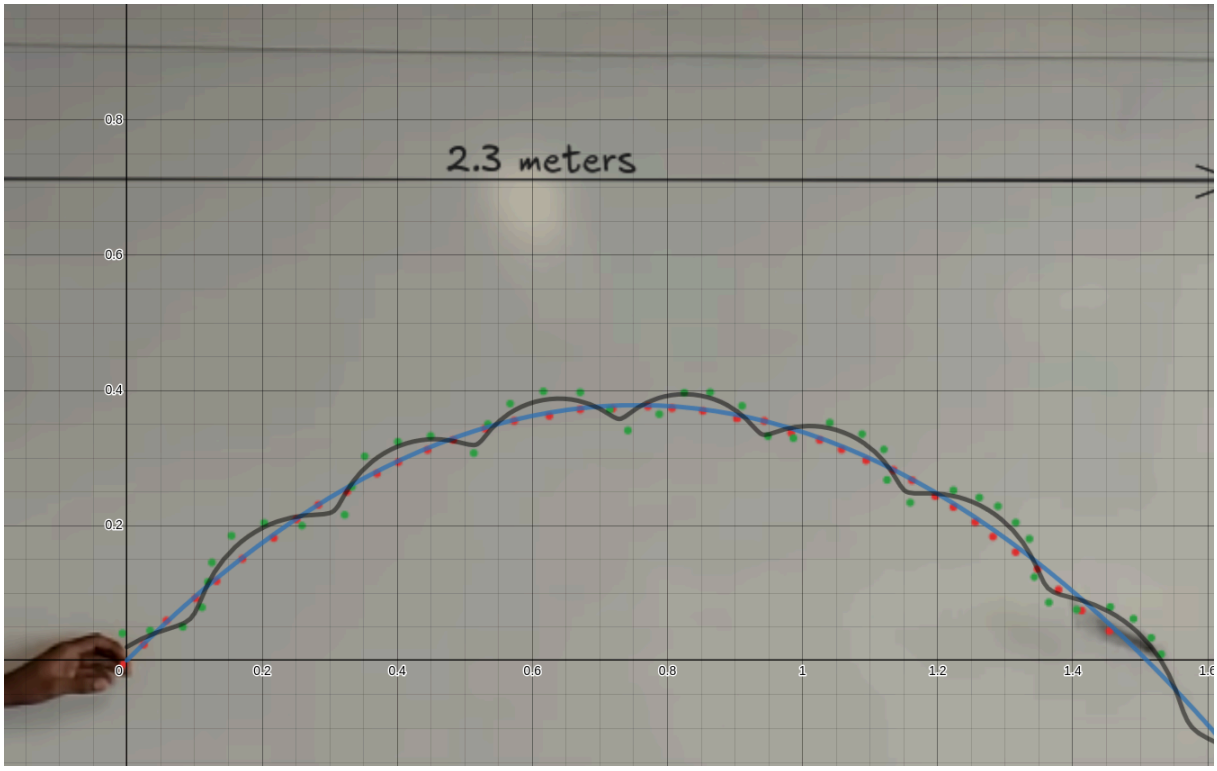

Figure 9: The experimental trace against the modelled flight path and tip path.

Here:

- The red dots are the traced flight path
- The blue line is our model's flight path
- The green dots are the traced tip path
- The black line is our model's tip path

For our model:

- $l = 0.013m = 13cm$
- $\hat{v} = 3.85$
- $\omega = 23.8 \text{ rad } s^{-1}$
- $\theta = 45°$

We can see overall, our model is quite accurate. There are two noticeable discrepancies though.

First of all, towards $x = 1.4m$, the model begins to overpredict the flight path. This is most likely because we did not take into account for air resistance against the pen.

Second of all, the cycloidal motion of the pens tip is underpredicted by the model. This can be caused by an inaccurate angular frequency determined which would lead to propagating errors in our model. Angular frequency will also fall very slightly due to air resistance.

Furthermore, in our experiment, the pen is not perfectly balanced at the centroid, which would also cause deviations from our models.

Thus, through experimental verification, we can conclude that our model is accurate enough to represent the motion of a throwing knives tip in flight.

3. Conclusion

3.1. Summary of Findings

Our mathematical model successfully derives a vector-valued function describing a knife's rotating tip during flight, with time-based parameterization enabling dynamic motion analysis. The framework handles varying initial conditions while accurately representing cycloidal motion, validated through experimental verification.

Mathematical analysis proved valuable in correcting physical intuitions, particularly in revising our understanding from assumed sinusoidal motion to actual cycloidal behavior. This demonstrates the importance of rigorous mathematical derivation in physical modeling.

3.2. Evaluation of Model

The model operates under theoretical constraints affecting real-world application, including simplified assumptions about air resistance and angular momentum. Perfect centroid balance and two-dimensional motion restrictions, while mathematically convenient, limit the model's ability to capture complete throwing dynamics.

Experimental verification revealed discrepancies, particularly in flight path endings and cycloidal motion magnitude. However, these limitations only define the model's scope rather than invalidating its fundamental approach.

3.3. Further Developments

Future development should focus on three-dimensional space modeling, incorporating compound rotations across multiple planes. This would better reflect real-world throwing complexity and enable analysis of off-axis rotation relative to flight paths.

Practical applications could be enhanced by developing blade angle calculations and exploring impact dynamics through vector calculus. These additions would improve our understanding of successful throwing mechanics.

The model could be refined by incorporating air resistance and analyzing angular momentum conservation. Investigation of mass distribution and torque effects would bridge theoretical and practical applications, creating a more comprehensive framework for knife throwing analysis.

The proposed enhancements would strengthen both the model's mathematical sophistication and its practical utility in improving throwing technique. This integration would provide a more complete understanding of this complex physical system.